A case of equine multicentric lymphoma: Clinical, microscopical, and molecular findings

Gabriela Fernandes Silva[1] (iD), Tiago Esteves Ribeiro[1,2], Raquel Cunha[1,2,3], Patricia Becerra Salas[1,2], Tiago Guimarães[1,2,3], Mário Ribeiro[1], Gonçalo Barros[1], Fátima Carvalho[1], João Rodrigo Mesquita[1,4,5] (iD) and Irina Amorim[1,6,7]* (iD)

[1]ICBAS School of Medicine and Biomedical Sciences, Porto University, Porto, Portugal
[2]Equine Clinical Centre of Vairão (CCEV), Vairão, Portugal
[3]AL4animals, Associate Laboratory for Animal and Veterinary Sciences, Lisbon, Portugal
[4]Epidemiology Research Unit (EPIUnit), Institute of Public Health of the University of Porto, Porto, Portugal
[5]Laboratory for Integrative and Translational Research in Population Health (ITR), Porto, Portugal
[6]Institute of Molecular Pathology and Immunology of the University of Porto (IPATIMUP), Porto, Portugal
[7]Institute for Research and Innovation in Health (i3S), Porto, Portugal

Abstract

Background: Although relatively uncommon, lymphoma is the most prevalent haematopoietic neoplasia in horses, and multicentric lymphoma remains the most common presentation of the disease. The pathogenesis of equine lymphoma is still poorly understood and the diagnosis is usually confirmed at an advanced stage of the disease, compromising the prognosis. This study investigated the clinical, pathological, and molecular features of a case of equine multicentric lymphoma.

Case Description: An apparently healthy 5-year-old crossbreed mare hospitalized at the Centre of Animal Reproduction of Vairão, Portugal, suddenly presented clinical signs of supraorbital oedema and mandibular lymph node enlargement, developing fever, facial oedema, and generalized lymphadenopathy. The mare ended up dying twenty-four days after the first clinical signs due to multisystem organ failure. Haematological and biochemical analyses, necropsy, and microscopic and molecular evaluation of affected tissues were performed. At necropsy, the main findings were multiple multinodular lesions, distributed along the serous surface of oropharynx, trachea, pericardium, gastrointestinal tract, and mesentery. Microscopically, these consisted of solid proliferations of neoplastic round cells that exhibited immunopositivity for CD3 (T cells). Based on these findings, a medium-grade multicentric T-cell lymphoma was diagnosed.

Conclusion: There is still very little research regarding the molecular characterization of lymphoma in horses. As an entity itself is quite heterogeneous, it is important to describe the interspecies particularities to understand its development and behaviour.

Keywords: Equine, Horse, Lymphoma, Multicentric, T-cell.

Introduction

Lymphoma is a haematopoietic neoplasia that represents a heterogeneous group of malignancies originating in lymphoid tissue (lymph nodes, spleen, and gut-associated lymphoid tissue) (Taintor and Schleis, 2011). Although haemolymphatic tumours in horses are relatively uncommon, lymphoma is the most prevalent haematopoietic neoplasia in this species (Meyer *et al*., 2006).

Based on anatomical location, lymphoma can be classified as multicentric, alimentary, mediastinal, cutaneous, and solitary (extranodal) (Miglio *et al*., 2019). In horses, multicentric lymphoma is the most frequent, followed by alimentary lymphoma, which remains the most common intestinal neoplasm in this species (Miglio *et al*., 2019). Although less common, lymphomas of the upper airways, central nervous system, heart, adrenal glands, reproductive organs, and eyes have also been reported (Taintor and Schleis, 2011). Lymphoma immunophenotyping allows the characterization of neoplastic cell histogenesis as B cells, T cells, and Natural Killer cells, and according to a retrospective study, T-cell-rich large B-cell lymphoma (TCRLBC) is the most common lymphoma subtype in horses (Durham *et al*., 2013).

The pathogenesis of equine lymphoma is still poorly understood. There is no apparent breed or sex predilection. Any age can be affected, however, a greater predisposition for horses with 5–10 years of age is reported (Meyer *et al*., 2006; Durham *et al*., 2013).

In horses, clinical signs common to all forms of lymphoma include weight loss, depression, lethargy, swelling of the ventral body wall or distal limbs, recurrent fever, and lymphadenopathy (Taintor and Schleis, 2011). Clinical signs of lymphoma are generally the result of the dysfunction of the affected organs, and the course of the disease is typically rapid, whereby the clinical manifestation tends to be evident at a late stage (Germann *et al*., 2008). The associated laboratory findings in horses with lymphoma reflect a high frequency of abnormalities, namely anaemia, thrombocytopenia, hyperfibrinogenaemia, hypoalbuminaemia, and hyperglobulinaemia (Meyer *et al*., 2006).

In horses with suspected lymphoma, the diagnosis involves physical examination, focusing on the evaluation of superficial and deep lymph nodes evaluation and thoracic and abdominal ultrasound, to observe images suggestive of neoplastic transformation. Definitive diagnosis is made through the identification of neoplastic lymphocytes in tissues, fluids, or peripheral blood. Histopathological examination remains the most accurate method for diagnosing this disease (Ness, 2016).

The prognosis of all forms of lymphoma is poor. Nevertheless, to prolong the survival time, surgical excision, radiation, and chemotherapy are available as palliative therapies in horses (Ness, 2016).

In this report, we describe the clinical, laboratory, and histopathological findings of a 5-year-old mare diagnosed with multicentric lymphoma.

Case Details

On 30th of August 2022, a 5-year-old crossbreed mare was hospitalized at the Centre of Animal Reproduction of Vairão, Portugal, for routine reproductive procedures. On physical examination, supraorbital oedema and enlargement of the mandibular lymph nodes were detected. Therefore, due to suspicion of an anaphylactic reaction, a single dose of intravenous (IV) Diurizone® (dexamethasone and dihydrochlorothiazide) was administered, and on the next day, IV flunixin-meglumine (1.1 mg/Kg; SID) was provided following an episode of slight hyperthermia.

Six days later, the facial swelling increased involving the masseteric region that displayed a positive godet sign, but without any signs of pain or discomfort on palpation. No signs of dysphagia, purulent nasal discharge, or enlarged guttural pouches were observed. Ultrasound examination of the head confirmed oedema and lymphadenopathy. Radiographic projections of the head and endoscopy of the upper airways were also performed, which did not reveal any other alterations. Consecutive haematological and biochemical analyses

were performed, whose alterations are summarized in Table 1. Due to the suspicion of an infectious condition, a continuous therapeutic protocol was started with intramuscular (IM) procaine penicillin (22,000 IU/Kg; BID) and IV flunixin-meglumine (1.1 mg/Kg; SID), and IV gentamicin (6.6 mg/Kg; SID) was administered for 3 days.

On the 13th of September, the mare presented a slight decrease on facial oedema. Fine needle aspiration of the enlarged mandibular lymph node was performed for cytological examination which revealed cellular pleomorphism of the myeloid and lymphoblastic cell lineage. At this point, the biochemical parameters revealed hyperproteinaemia, hyperglobulinaemia, and hypoalbuminaemia. A proteinogram was requested and the results showed a monoclonal gammopathy consistent with hypergammaglobulinemia (Fig. 1). The clinical situation was explained to the owner, who despite this, decided to voluntarily discharge the animal, with medical indication of antibiotic and anti-inflammatory treatment.

The mare returned on the 22nd of September with prostration, fever, dyspnoea, lack of appetite, severe weight loss, dehydration, and pronounced oedema and lymphadenopathy of the head. At physical examination, increased capillary refill time (3 seconds), tachycardia (72 bpm), and tachypnoea (32 rpm) were noted. There was no positive jugular pulse and intestinal motility was greatly diminished. Abdominal ultrasound and rectal palpation ruled out colic. At this point, haematology and biochemistry revealed severe thrombocytopenia with alterations in most biochemical parameters (decreased albumin/globulin ratio, increased urea, creatine kinase, and iron, and decreased gamma-glutamyl transferase). A fluid therapy protocol with Ringer's Lactate via IV supplemented with 2 l of colloid was implemented and the previous temperature and antibiotic therapy protocol was maintained. Despite the treatment efforts, the mare's body temperature reached peaks of 40.2°C and from then on, the mare failed to clinically respond to antipyretics. Thoracic, abdominal, and cardiac ultrasounds were performed, revealing an atypical image of the cardiac silhouette at the level of the 4–6th left intercostal spaces, characterized by an irregular border and thickening of the cardiac wall (Fig. 2). With no improvement of the clinical condition, the mare collapsed on 24th of September, and the corpse was subjected to necropsy examination.

At necropsy, oedema of the subcutaneous tissue, generalized lymphadenopathy, and the presence of multiple white to brownish multinodular, partially encapsulated, well-delimited masses of moderately firm consistency were observed, measuring between 0.5 and 8 cm in their longest axis, diffusely distributed over the serous surface of several organs, namely the oropharynx, trachea, pericardium, mesentery, and gastrointestinal tract (Fig. 3). In the thoracic cavity, white foam filled the tracheal lumen, the nasopharynx, and the nasal cavity, and a collection of reddish translucent

Table 1. Abnormalities of haematological and biochemical parameters.

		Analysis date				
		05/09/22	13/09/22	22/09/22	23/09/22	Reference
Haematology	Leukocytes (×10³/ul)	30.93 ↑	22.28 ↑	14.82 ↑	11.76	5.4–14.3
	Neutrophils (×10³/ul)	11.44 ↑	5.94	5.19	6.22	2.3–9.6
	Lymphocytes (×10³/ul)	18.87 ↑	12.52 ↑	7.56	4.21	1.5–7.7
	Monocytes (×10³/ul)	0.62	3.19 ↑	2.07 ↑	1.25	0.0–1.5
	MCHC (g/dl)	39.1 ↑	38.9 ↑	43.3 ↑	40.6 ↑	31.0–38.6
	RDW %	27.6 ↑	26.1	29.9 ↑	26.0	12.0–27.0
	Total platelets (×10³/ul)	192	161	69 ↓	18 ↑	90.0–350.0
Biochemistry	Total protein (g/dl)	9.44 ↑	9.52 ↑	10.37 ↑	9.42 ↑	5.2–7.6
	Albumin (g/dl)	2.48 ↓	1.82 ↓	1.22 ↓	1.10 ↓	2.6–4.1
	Globulins (g/dl)	6.96 ↑	7.70 ↑	9.15 ↑	8.32 ↑	2.6–4.0
	Urea (mg/dl)	33.2	34.0	99.7 ↑	78.8 ↑	24.0–58.0
	ASAT (U/l)	101.9 ↑	78.5 ↓	380.5	306.3	152.0–412.0
	GGT (U/l)	7.6	<3.0 ↓	3.4 ↓	3.3 ↓	6.0–32.0
	Creatine kinase (U/l)	131.9	135.8	1086.4 ↑	431.4 ↑	60.0–333.0
	Iron (ug/dl)	122.4	162.7 ↑	141.6 ↑	129.6	73.0–140.0

MCHC: mean corpuscular haemoglobin concentration; RDW: red cell distribution width; ASAT: aspartate transaminase; GGT: gamma-glutamyl transferase.
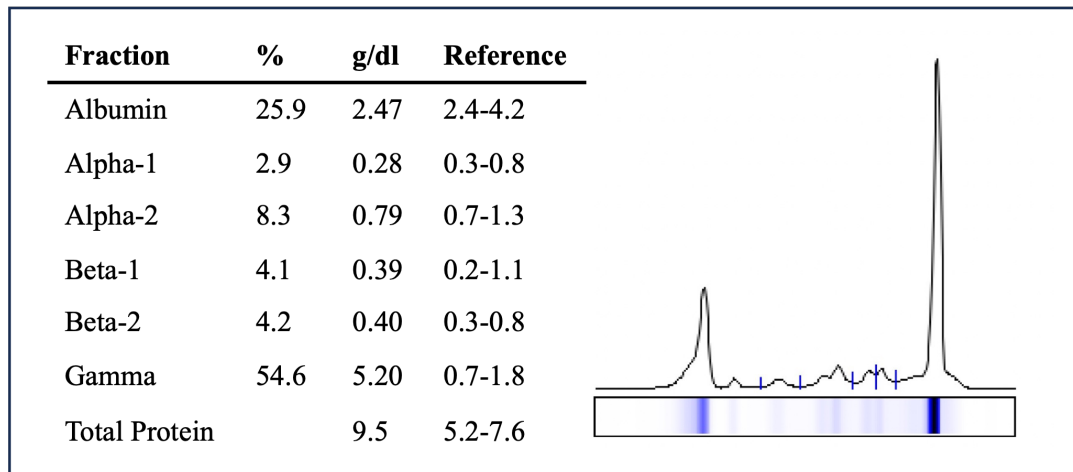

Fraction	%	g/dl	Reference
Albumin	25.9	2.47	2.4-4.2
Alpha-1	2.9	0.28	0.3-0.8
Alpha-2	8.3	0.79	0.7-1.3
Beta-1	4.1	0.39	0.2-1.1
Beta-2	4.2	0.40	0.3-0.8
Gamma	54.6	5.20	0.7-1.8
Total Protein		9.5	5.2-7.6

Fig. 1. Proteinogram suggesting monoclonal hypergammaglobulinemia.

fluid was observed in the pleural space. The right atrial wall was thickened and petechiae were present on the visceral pleura, diaphragm, and cardiac surface. In the abdominal cavity, a build-up of yellowish translucent fluid was observed in the peritoneal cavity and the transverse abdominal muscle appeared darkened and friable. Representative samples of the various masses, lymph nodes, lungs, diaphragm, heart, gastrointestinal tract, and abdominal transverse muscle were collected and fixed in 10% neutral buffered formalin.

Tissue samples were routinely processed, paraffin-embedded, and 2 μm thick serial sections were cut and stained with haematoxylin and eosin (H&E) for histopathological evaluation. The several masses presented identical histological features, consisting of multinodular neoplastic lesions with poorly defined borders, composed of dense proliferation of round cells arranged in a diffuse or solid pattern, supported by a scarce extracellular matrix (Fig. 4a). The neoplastic cells had round, ovoid, or sometimes kidney-shaped nuclei, with high pleomorphism, lumpy chromatin,
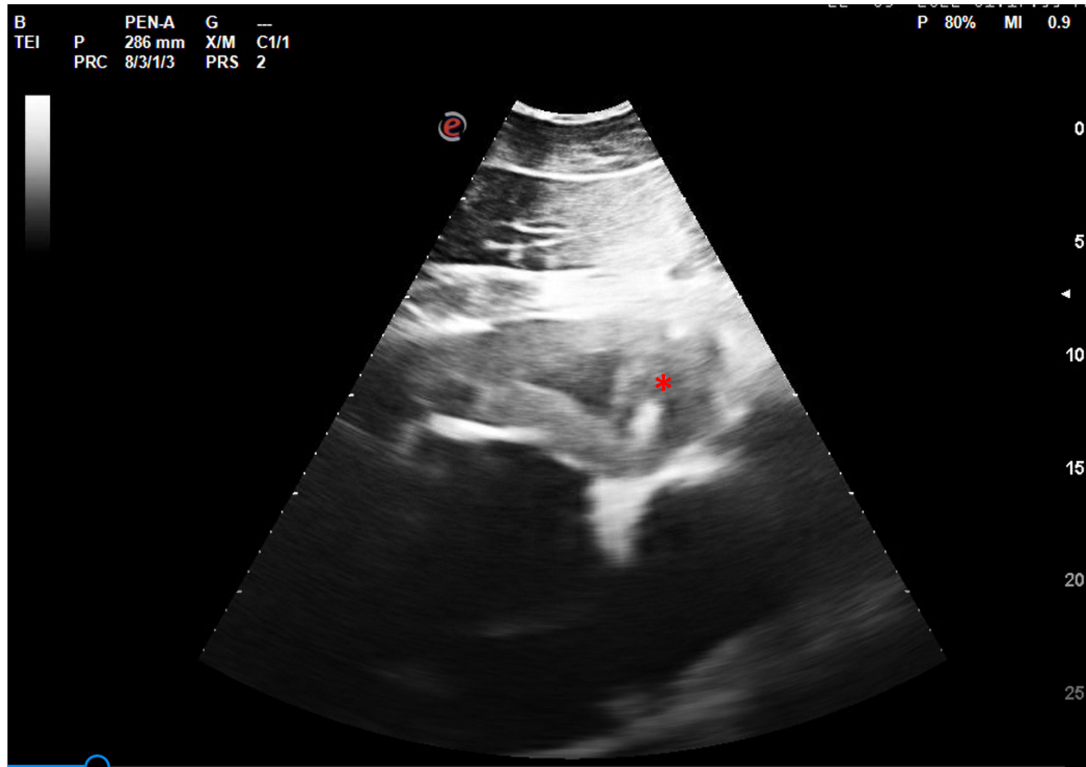
Fig. 2. Ultrasound image of the heart showing irregular border and thickening of the left ventricle wall (*).

at least two prominent nucleoli and variable amount of acidophilic cytoplasm. It was possible to observe numerous multinucleated cells (Fig. 4b). The neoplastic cells were present in the lymph nodes, infiltrating adjacent muscle and adipose tissue, as well as in the heart (Fig. 4e), diaphragm and peritoneum. Mitotic activity was counted in ten high power fields (HPFs) and the average result reached at least 6 mitoses/HPF. Additionally, a histological examination of the lungs revealed subacute to chronic interstitial pneumonia and the presence of bacterial organisms with a rod-like morphology, pulmonary oedema, and congestion.

To characterize the histogenesis and the immunophenotype of the neoplastic cells, immunohistochemistry (IHC) was performed. Tissue sections of neoplastic masses, lymph nodes, and heart were deparaffinized and hydrated, and antigen retrieval was performed in a water bath with a Target Retrieval solution (Dako, Santa Clara, CA). The Novolink™ Max-Polymer detection system (Novocastra, Newcastle, UK) was used for visualization, according to the manufacturer's instructions. The slides were incubated overnight at 4°C in a humid chamber with polyclonal anti-CD3 antibody (Dako), anti-CD79α (clone HM57, Leica Biosystems), anti-CD20 (clone L26, Dako), anti-Ki67 (clone MIB-1, Dako), anti-PD-L1 (clone ab233482, abcam), and anti-C-KIT (clone CD117, Leica Biosystems). Sections were washed with triphosphate-buffered saline at each step of the procedure. The stain was developed with 3,3-diamino-benzidine (DAB; Sigma, St. Louis, MO) and the sections were counterstained with haematoxylin, dehydrated, and mounted. Positive and negative immunohistochemical controls were included. More than 85% of neoplastic cells showed cytoplasmic immunostaining for CD3 (T cells) (Fig. 4c), and CD20 presented cytoplasmic immunoreactivity in about 5% of cells (B cells) (Fig. 4d). The CD20 marker was selected instead of CD79α due to its superior labelling quality in equine lymphocytes, as previously reported by Durham *et al*. (2013). Ki-67 proliferative index reached 19% (evaluated by the ratio of positively stained nuclei to at least 1,000 nuclei analysed in the regions of highest expression (hotspots)). No immunostaining for PD-L1 and C-KIT antibodies was detected.

According to the anatomical location and distribution of the lesions, along with the histological and immunohistochemical results, the mare was diagnosed with a medium-grade multicentric T-cell lymphoma.

Paraffin-embedded lung and neoplastic tissue samples cut at 10 μm were processed for DNA extraction using the EXTRACTME® DNA tissue kit (Blirt, Trzy Lipy, Poland) according to the manufacturer's instructions. A seminested polymerase chain reaction (PCR) targeting a 230 bp region of the glycoprotein B of Equid Herpesvirus 5 (EHV-5) was performed as previously described (Marenzoni *et al*. 2010). Briefly, a total of 2 μl of genomic DNA was added to 12.5 μl of

Fig. 3. Macroscopic findings of the mare submitted to necropsy. (a) Lymphadenopathy of the mandibular lymph nodes; (b) and (c) Cross-section of multiple and well-circumscribed multinodular lesions located in the submandibular region; (d) and (e) Lesions and petechiae distributed along the serous surface of diaphragm, pericardium, and heart; (f) Petechiae and oedema in the gastrointestinal tract and mesentery and enlarged mesenteric lymph nodes.

Xpert Fast Hotstart Mastermix (2X) with dye (GRISP, Porto, Portugal), 8.5 µl of deionized sterile water, and 1 µl (10 µM) of primers in a 25.0 µl final volume of the reaction mixture. The reactions were carried out in an automatic DNA thermal cycler 100 (Bio-Rad), including negative (water) and positive controls. The PCR amplification products were visualized by Xpert green (Grisp, Porto, Portugal) fluorescence after electrophoresis in a 1.5% agarose gel at 100 V for 40 minutes. After the seminested PCR and electrophoresis, no amplified product of the expected size was visualized.

Discussion

Equine lymphoma is a heterogeneous disease with a variable presentation of clinical signs, laboratory parameters, and pathological findings (Meyer *et al*., 2006).

Lymphoma affects horses of all breeds and there is no apparent genetic predisposition for the development of this neoplasia. Nevertheless, reports of lymphoma in an aborted equine fetus and in two 1-year-old horses suggest that congenital alterations may be implicated in tumour development (Tomlinson *et al*., 1979; Haley and Spraker, 1983; Taintor and Schleis, 2011). Horses between 5 and 10 years of age are more predisposed to developing this neoplasia (Meyer *et al*., 2006; Durham

et al., 2013), which is in line with the current case description.

Multicentric lymphoma is the most frequent type of haematopoietic neoplasia of the horse, characterized by the generalized involvement of superficial and deep lymph nodes and diffuse involvement of other organs. In this case, in addition to the generalized involvement of the lymph nodes, the lymphoma extended to the muscles and adjacent adipose tissue, diaphragm, heart, and peritoneum, suggesting probable dissemination of neoplastic lymphocytes.

The risk factors for the development of equine lymphoma are unknown, as well as the presence of etiological factors (Miglio *et al*., 2019). The possible involvement of retroviral or corynebacterial infections in malignant transformation has been speculated, but results have been inconclusive (Sheahan *et al*., 1980; Vander and Davis, 2013). A recent study developed by Miglio *et al*. (2019) detected positivity for EHV-5 in lymphoma equine tissues. Given the association between EHV-5 and some forms of lymphoma (multicentric, cutaneous, and solitary) and the fact that the horse is a natural host for herpesvirus, viral involvement in equine lymphoma should be investigated (Vander and Davis, 2013). In this animal, PCR for EHV-5 was negative, possibly excluding this etiological agent.
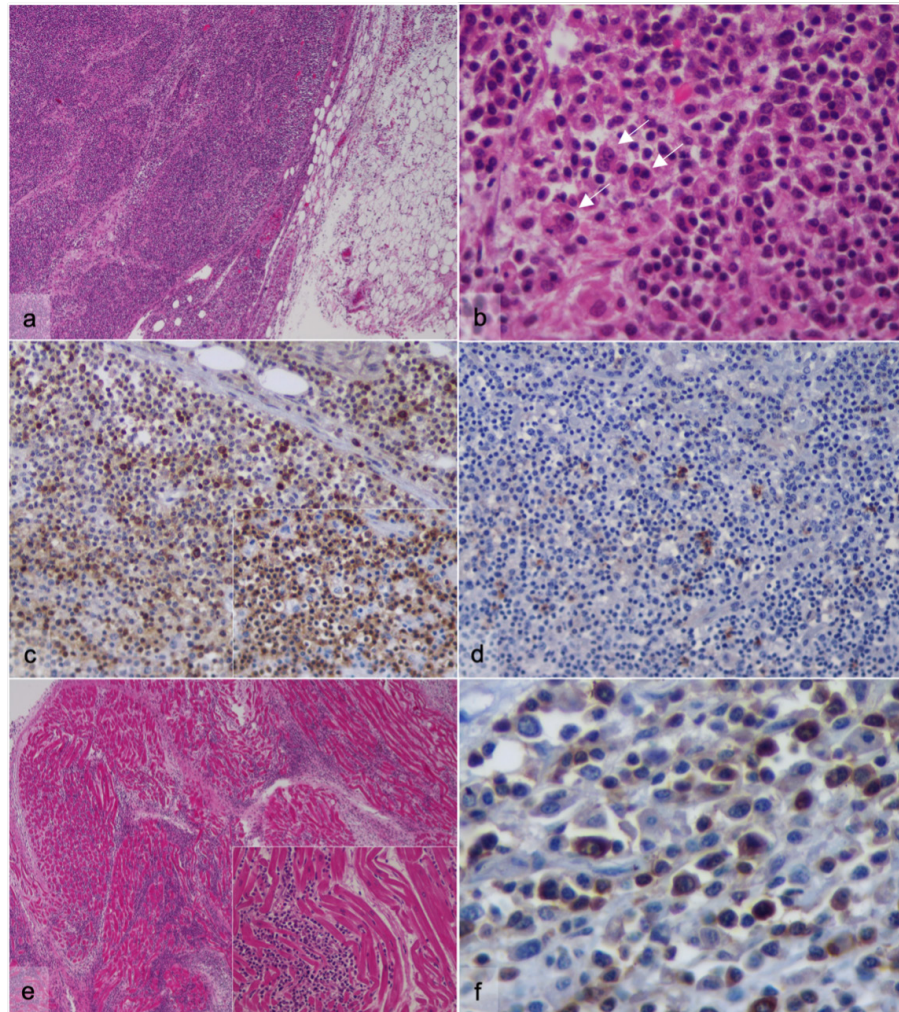
Fig. 4. Microscopic evaluation of the multinodular masses and heart. (a)–(d) Abdominal neoplastic formations; (a) Partially encapsulated neoplastic lesion composed of dense population of round cells (H&E, 100x); (b) Note the high pleomorphism of the neoplastic cells and the presence of numerous multinucleated cells (arrows) (H&E, 600x); (c) The majority of neoplastic cells express diffuse cytoplasmatic immunostaining for CD3 (DAB, 100x); Inset: cytoplasmatic and membranous CD3 positive staining (DAB, 400x); (d) Scattered lymphocytes expressing cytoplasmatic CD20 immunostaining (DAB, 100x). (e) and (f) Heart; (e) Diffuse infiltration of endocardium by neoplastic lymphocytes (H&E, 40x, 600x); (f) Lymphocytic infiltration of CD3 immunopositive cells (DAB, 600x).

Clinical signs in horses with lymphoma are often nonspecific, and depend on the organs affected (Ness, 2016). The first evident clinical signs presented by this mare were facial oedema, enlarged mandibular head lymph nodes, and recurrent fever, so different causes were considered. Lymphadenopathy is a common finding in horses with multicentric lymphoma (Ness, 2016). Enlargement of the lymph nodes of the head, namely the mandibular lymph nodes, is occasionally the result of sinusitis, guttural pouch disorders, or a response to generalized respiratory infections such as equine influenza, EHV-1 and EHV-4 or *Streptococcus*

equi subsp. *equi* (McGorum and Dixon, 2000). In this case, nasal discharge was not present, and the imaging studies did not reveal the presence of foreign bodies or other relevant abnormalities in the upper respiratory tract. After fever therapeutic ineffectiveness, other causes were investigated. Tumour necrosis, as well as the release of cytokines produced by the tumour or by reactive macrophages, can cause an increase in body temperature and justify the refractory response to antibiotics (Ness, 2016). In advanced stages of the disease, clinical signs reflect organ failure due to

invasion by neoplastic lymphocytes, with consequent tissue destruction and loss of function (Ness, 2016). Haematological and biochemical alterations are variable. In this case, neutrophilia was evident, probably in response to tumour necrosis and lymphocytosis (Meyer *et al*., 2006). Thrombocytopenia occurs less frequently, but its detection in late-stage disease may indicate immune-mediated destruction or infiltration of the bone marrow (Ness, 2016). In this animal, the most evident biochemical alterations during the course of the disease were hyperglobulinemia and hypoalbuminemia, concordant findings in animals with lymphoma. Hyperglobulinemia may reflect a systemic inflammatory response to tumour necrosis (Ness, 2016), a paraneoplastic process or atypical antibodies generated by neoplastic lymphocytes (Wensley *et al*., 2023). It may also result in down-regulation of albumin synthesis, which may also be diminished by inadequate intake and absorption of nutrients (Wensley *et al*., 2023). The proteinogram revealed a monoclonal gammopathy due to the overproduction of immunoglobulins, suggestive of lymphoid neoplasia. A recent study on equine lymphoma performed by Wensley *et al*. (2023) associated high concentrations of globulin with decreased survival time, suggesting that hyperglobulinemia acts as a negative prognostic factor in this disease. Hyperfibrinogenaemia is a common laboratory finding in horses with lymphoma (Meyer *et al*., 2006) however, this parameter was not evaluated in this animal.

Histopathologically, lymphomas are generally heterogeneous, and the morphology of neoplastic lymphocytes is variable, making it often difficult to distinguish between reactive cells and well-differentiated neoplastic cells (Rendle *et al*., 2012). In this case, infiltration of macrophages and multinucleated cells was observed, consistent with previous reports (Ueno *et al*., 2012). Multinucleated giant cells are a common finding in equine lymphoma biopsies and were previously associated with T cell-derived lymphomas (Ueno *et al*., 2012). It was hypothesized that neoplastic T lymphocytes produce interferon gamma that may result in macrophage activation and the formation of multinucleated cells (Ueno *et al*., 2012). The mitotic count predicts the grade of lymphoma, which can be indolent, low-, medium-, or high-grade (Durham *et al*., 2013). In this case, the lymphoma was classified as medium grade (6 to 10 mitoses/HPF).

IHC enables the determination of the immunophenotype of neoplastic lymphocytes. In this case, although few positive B cells were observed within the neoplastic population, the great majority of the neoplastic lymphocytic population was CD3 positive, assigning its origin to T cells and allowing the diagnosis of T-cell lymphoma. In a retrospective study carried out by Durham *et al*. (2013) in 203 horses with lymphoma classified according to the World Health Organization (WHO) classification system, TCRBCL was the most common phenotype in horses (43%), followed by peripheral T-cell lymphoma (22%), and the multicentric form is usually related to these two phenotypes (Durham *et al*., 2013). Although not yet fully clarified in horses, T-cell lymphoma is generally more aggressive and has a poorer prognosis when compared to B-cell lymphoma (Taintor and Schleis, 2011). Furthermore, the multicentric and mediastinal forms were also associated with decreased survival time compared to other locations (Wensley *et al*., 2023). Regardless of lymphoma subtype, the prognosis is poor, and the survival time is variable and depends on the extension of the disease and organs involved (Ness, 2016). Due to multi-organ failure, most horses with multicentric lymphoma are euthanized a few weeks to months after diagnosis (Meyer *et al*., 2006). In the present case, the mare ended up dying due to the worsening of the clinical picture, 24 days after the detection of the first clinical signs. The diagnosis of lymphoma is essentially established at an advanced stage of the disease, responses to treatment are variable and treatment is mainly palliative rather than curative (Taintor and Schleis, 2011). The WHO has established a clinical staging system for lymphoma in domestic animals (Vail *et al*., 2019). According to this proposed scheme, the current case should be classified at least as stage IIIb lymphoma, presenting with generalized lymph node involvement and systemic signs. However, bone marrow cytology was not performed, impairing a more accurate clinical staging of the neoplastic disease. Depending on the stage and progression of the disease, the treatment for lymphoma includes surgical excision of the tumour, radiotherapy, and chemotherapy, including several multi-drug protocols, already reported in horses (Taintor and Schleis, 2011).

Conclusion

Equine lymphoma presents unique and species-specific characteristics, presenting mostly as a multi-organ disease that can be difficult to diagnose given the non-specificity of clinical signs. In human medicine, it is well established that the morphology, immunophenotype, and molecular and clinical features, as well as their biological behaviour, allow the classification of lymphoma. In horses, information about these features is limited. As an entity itself quite heterogeneous, a better understanding and study of the development and behaviour of equine lymphoma allows to refine the establishment of diagnoses and therapeutic strategies, increasing survival time and improving prognoses.

processed samples, and extracted DNA. JRM performed the PCR analyses. IA critically revised the manuscript for important intellectual content. All authors read and approved the final manuscript.

References

Durham, A.C., Pillitteri, C.A., San Myint, M. and Valli, V.E. 2013. Two hundred three cases of equine lymphoma classified according to the World Health Organization (WHO) classification criteria. Vet. Pathol. 50(1), 86–93.

Germann, S.E., Richter, M., Schwarzwald, C.C., Wimmershoff, J. and Spiess, B.M. 2008. Ocular and multicentric lymphoma in a young racehorse. Vet. Ophthalmol. 11, 51–56.

Haley, P.J. and Spraker, T. 1983. Lymphosarcoma in an aborted equine fetus. Vet. Pathol. 20(5), 647–649.

Marenzoni, M.L., Coppola, G., Maranesi, M., Passamonti, F., Cappelli, K., Capomaccio, S., Verini Supplizi, A., Thiry, E. and Coletti, M. 2010. Age-dependent prevalence of equid herpesvirus 5 infection. Vet. Res. Communic. 34(8), 703–708.

McGorum, B.C. and Dixon, P.M. 2000. Clinical examination of the respiratory tract. Equine Respir. Med. Surg. 103–117.

Meyer, J., Delay, J. and Bienzle, D. 2006. Clinical, laboratory, and histopathologic features of equine lymphoma. Vet. Pathol. 43(6), 914–924.

Miglio, A., Morelli, C., Gialletti, R., Lauteri, E., Sforna, M., Marenzoni, M.L. and Antognoni, M. T. 2019. Clinical and immunophenotypic findings in 4 forms of equine lymphoma. Can. Vet. J. 60(1), 33–40.

Ness, S.L. 2016. Lymphoma. In Equine clinical immunology. Eds., Julia, M., Felippe, B., 1st ed., USA: John Wiley & Sons, Inc., pp: 181–191.

Rendle, D., Hughes, K., Farish, C. and Kessell, A. 2012. Multicentric T-cell lymphoma presenting as inferior palpebral swelling in a Standardbred mare. Aust. Vet. J. 90(12), 485–489.

Sheahan, B.J., Atkins, G.J., Russell, R.J. and O'Connor, J.P. 1980. Histiolymphocytic lymphosarcoma in the subcutis of two horses. Vet. Pathol. 17(2), 123–133.

Taintor, J. and Schleis, S. 2011. Equine lymphoma. Equine Vet. Educ. 23, 205–213.

Tomlinson, M.J., Doster, A.R. and Wright, E.R. 1979. Lymphosarcoma with virus-like particles in a neonatal foal. Vet. Pathol. 16(5), 629–631.

Ueno, T., Wada, S., Mashita, S., Kuwano, A. and Katayama, Y. 2012. pathological findings in a case of equine T-cell lymphoma associated with ataxia. J. Equine Vet. Sci. 32(6), 315–319.

Vail, D.M., Thamm, D.H. and Liptak, J.M. 2019. Hematopoietic tumors. Withrow MacEwen's Small Anim. Clin. Oncol. 2019, 688–772.

Vander Werf, K. and Davis, E. 2013. Disease remission in a horse with EHV-5-associated lymphoma. J. Vet. Inter. Med. 27(2), 387–389.

Wensley, F.M., Berryhill, E.H. and Magdesian, K.G. 2023. Association of globulin concentrations with prognosis in horses with lymphoma. Front. Vet. Sci. 9, 1086010.